Are your MRI contrast agents cost-effective?
Learn more about generic Gadolinium-Based Contrast Agents.
FRESENIUS KABI
caring for life

AJNR

A New Frontier in Temporal Bone Imaging: Photon-Counting Detector CT Demonstrates Superior Visualization of Critical Anatomic Structures at Reduced Radiation Dose

J.C. Benson, K. Rajendran, J.I. Lane, F.E. Diehn, N.M. Weber, J.E. Thorne, N.B. Larson, J.G. Fletcher, C.H. McCollough and S. Leng

This information is current as of April 16, 2024.

AJNR Am J Neuroradiol 2022, 43 (4) 579-584
doi: https://doi.org/10.3174/ajnr.A7452
http://www.ajnr.org/content/43/4/579

A New Frontier in Temporal Bone Imaging: Photon-Counting Detector CT Demonstrates Superior Visualization of Critical Anatomic Structures at Reduced Radiation Dose

J.C. Benson, K. Rajendran, J.I. Lane, F.E. Diehn, N.M. Weber, J.E. Thorne, N.B. Larson, J.G. Fletcher, C.H. McCollough, and S. Leng

ABSTRACT

BACKGROUND AND PURPOSE: Photon-counting detector CT is a new technology with a limiting spatial resolution of ≤150 μm. In vivo comparisons between photon-counting detector CT and conventional energy-integrating detector CT are needed to determine the clinical impact of photon counting-detector CT in temporal bone imaging.

MATERIALS AND METHODS: Prospectively recruited patients underwent temporal bone CT examinations on an investigational photon-counting detector CT system after clinically indicated temporal bone energy-integrating detector CT. Photon-counting detector CT images were obtained at an average 31% lower dose compared with those obtained on the energy-integrating detector CT scanner. Reconstructed images were evaluated in axial, coronal, and Pöschl planes using the smallest available section thickness on each system (0.4 mm on energy-integrating detector CT; 0.2 mm on photon-counting detector CT). Two blinded neuroradiologists compared images side-by-side and scored them using a 5-point Likert scale. A post hoc reassignment of readers' scores was performed so that the scores reflected photon-counting detector CT performance relative to energy-integrating detector CT.

RESULTS: Thirteen patients were enrolled, resulting in 26 image sets (left and right sides). The average patient age was 63.6 [SD, 13.4] years; 7 were women. Images from the photon-counting detector CT scanner were significantly preferred by the readers in all reconstructed planes ($P < .001$). Photon-counting detector CT was rated superior for the evaluation of all individual anatomic structures, with the oval window (4.79) and incudostapedial joint (4.75) receiving the highest scores on a Likert scale of 1–5.

CONCLUSIONS: Temporal bone CT images obtained on a photon-counting detector CT scanner were rated as having superior spatial resolution and better critical structure visualization than those obtained on a conventional energy-integrating detector scanner, even with a substantial dose reduction.

ABBREVIATIONS: EID = energy-integrating detector; PCD = photon-counting detector

Photon-counting detector (PCD) CT is an emerging technology that has substantial promise in improving clinical imaging.[1,2] Conventional CT scanners are equipped with energy-integrating detectors (EIDs) that use a scintillator to convert x-rays into visible light, which a photodiode converts to an electric signal. EID-CT requires the use of septa between detector elements, which limit spatial resolution.[3] One CT manufacturer increased the available spatial resolution of the system by using attenuating filters to reduce the effective pixel aperture;[4] this use results in a decreased geometric dose efficiency, which requires an increase in the radiation dose to achieve the same noise level as an image without an attenuating filter (at lower spatial resolution). PCDs, conversely, directly transform photons into electric signal and record each individual photon and do not require septa between detector elements or the use of attenuating filters.[5] Hence, PCDs allow more dose-efficient high-spatial-resolution imaging.[6,7] In addition, the PCD assigns uniform weighting to each detected photon irrespective of its energy,[8] which results in an improved SNR. PCD-CT also provides decreased beam-hardening artifacts[9,10] and reduced electronic noise.[1,11]

Zhou et al[12] have previously demonstrated, in a cadaver study, that the lack of attenuating filters with PCD-CT can result in an approximately 50% dose reduction if other acquisition parameters are kept unchanged. PCD-CT can also improve visualization of key anatomic structures, which may improve clinical

Received December 18, 2021; accepted after revision January 9, 2022.

From the Departments of Radiology (J.C.B., K.R., J.I.L., F.E.D., N.M.W., J.E.T., J.G.F., C.H.M., S.L.) and Quantitative Health Sciences (N.B.L.), Mayo Clinic, Rochester, Minnesota.

J.C. Benson and K. Rajendran contributed equally to this work.

Drs McCollough and Fletcher receive industry funding to their institution from Siemens, which includes in-kind support for the evaluated equipment.

Please address correspondence to John C. Benson, MD, Department of Radiology, Mayo Clinic, 200 First St SW, Rochester, MN 55905; e-mail: Benson.John3@mayo.edu

Indicates article with online supplemental data.

http://dx.doi.org/10.3174/ajnr.A7452

diagnoses. On the basis of preliminary work,[13] we designed a temporal bone PCD-CT protocol that uses up to 31% lower radiation dose and a reconstruction kernel with 35% higher cutoff spatial frequency compared with EID-CT with an attenuating filter, and a 0.2-mm section thickness, which is half of that used at EID-CT (0.4 mm). The purposes of this pilot study were to compare the capabilities of a PCD-CT system with EID-CT with an attenuating filter for temporal bone imaging and to provide examples of PCD-CT temporal bone imaging in patients with clinical indications.

MATERIALS AND METHODS

Patient Cohort

Patients referred for a clinically indicated temporal bone CT examination scanned using EID-CT scanners were prospectively recruited to undergo a research temporal bone CT scan on an investigational PCD-CT system. Written informed consent was obtained from all participants for this Health Insurance Portability and Accountability Act–compliant, institutional review board–approved study (Mayo Clinic, Rochester, MN, USA). Relevant clinical data, including but not limited to temporal bone surgical history and findings on the clinical EID-CT, were abstracted from the electronic medical record.

CT Protocol

EID-CT scans were performed on a third-generation EID-CT system (SOMATOM Force; Siemens) using a ultra-high-resolution mode (120 kV; mean volume CT dose index = 51.5 [SD, 3.8] mGy; pitch = 0.35, rotation time = 1 second), according to our routine clinical protocol, which uses a Ur77 reconstruction kernel and 0.4-mm section thickness (the minimal section thickness for this CT system).[11] The ultra-high-resolution protocol uses an attenuating filter.

The research PCD-CT scan was performed on an investigational PCD-CT system (SOMATOM Count Plus; Siemens; 120 kV, mean volume CT dose index = 35.6 [SD, 1.7] mGy, pitch = 1.0–1.2, rotation time = 1 second) using the high-resolution mode (120 × 0.2 mm collimation) with a dedicated sharp Hr84 kernel and the smallest section thickness of 0.2 mm that is not possible on the EID-CT system. The in-plane detector pixel size of the PCD-CT system is 0.275 mm,[3,14,15] which translates to 0.151 mm at the isocenter. PCD-CT scans were performed at a 31% lower radiation dose compared with EID-CT (mean volume CT dose index = 35.6 versus 51.5 mGy). The dose-reduction factor for PCD-CT was determined by using phantom experiments and previously reported data[13] that showed lower image noise on PCD-CT relative to EID-CT when the section thickness and kernel are matched between the 2 systems.

Image Review

CT images were reconstructed in axial, coronal, and Pöschl planes using the smallest available section thickness (0.2 mm for PCD-CT and 0.4 mm for EID-CT). Two neuroradiologists, each with >10 years of experience (J.I.L. and F.E.D.), independently evaluated paired PCD-CT and EID-CT images on a 2-monitor workstation (syngo via; Siemens).

The images on the viewing workstation were arranged in 2 rows of 3 panels on each of the 2 monitors, with a subject's right temporal bone on the left monitor and the left temporal bone on the right monitor. Axial, coronal, and Pöschl plane images from EID-CT or PCD-CT were randomly assigned to either the upper or lower row, with all information relating to the scanner type, acquisition settings, or image-reconstruction parameters hidden from the reader. For each temporal bone side, readers were instructed to compare the upper and lower rows for each imaging plane, evaluating the visualization of each of 7 critical anatomic structures. Readers were allowed to pan and zoom as needed, as well as to double-click on any image so that it filled the monitor for closer inspection.

Specific directions were provided regarding the plane that should be used to evaluate each anatomic structure: axial plane, round window, incudomalleolar joint, modiolus; coronal plane, oval window, scutum; Pöschl plane, modiolus; incudostapedial joint. If present, ossicular prostheses were evaluated in the best visualized plane.

Images on the lower row were scored using a 5-point Likert scale: 1 = inferior resolution with degraded visualization, 2 = slightly inferior resolution without affecting visualization, 3 = equivalent resolution and visualization, 4 = slightly superior resolution without affecting visualization, and 5 = superior spatial resolution with improved visualization. Readers were encouraged to make free text comments. After all anatomic structures were scored, an overall image-quality score considering image sharpness, noise level, and artifacts was provided using the 5-point Likert scale.

Additional oblique reformatted images were created by a non-reader neuroradiologist (J.C.B.) to demonstrate certain anatomic structures: the ossicles, ossicular prostheses, and otosclerosis. These images were not used by the readers as part of the formal side-by-side PCD-to-EID comparison and, therefore, were not scored; they were created for illustrative purposes only.

Statistical Analysis

The Likert visualization scores of anatomic structures and the overall image-quality scores for each temporal bone reflected the comparative image quality, with a score of 3 indicating equivalent image quality between the scored (lower) image and the reference (upper) image. Scores of 1 and 5 represented cases in which one scanner type demonstrated definite improvement in spatial resolution and visualization or image quality relative to the other scanner type. Post hoc, the scores were reassigned such that they reflected PCD-CT impressions relative to clinical routine EID-CT.

The mean scores for the 2 readers were calculated for each evaluated critical structure. A 1-sample Wilcoxon rank-sum test of the overall image quality score was performed to test for significant asymmetry of the Likert scores with respect to a score of 3 (equivalence) using the mean scores of the readers. Comparisons were performed for individual readers and anatomic structures in each plane and across readers and structures. No adjustment was performed for the left and right temporal bones in the same patient. A P value $\leq$ .05 was considered significant under a 2-

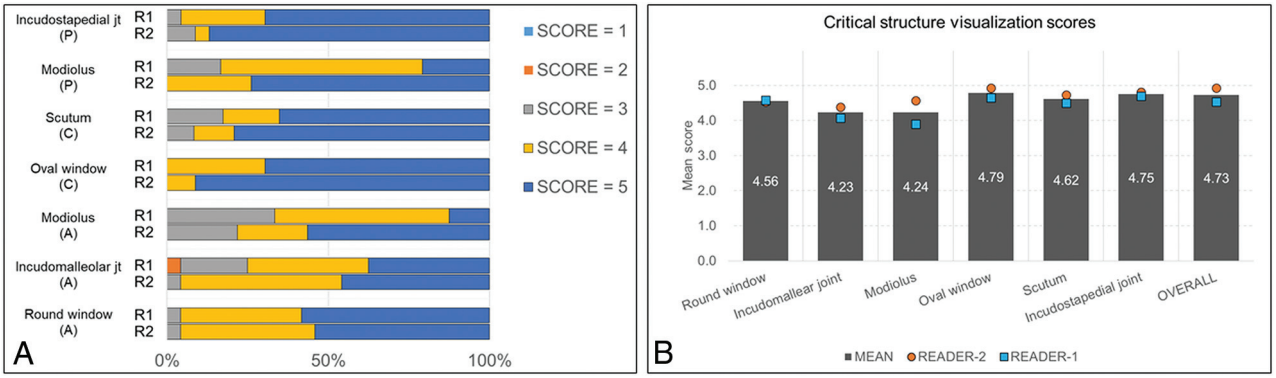

FIG 1. Readers' score distribution for spatial resolution and visualization of critical anatomic structures in different reformatted planes (*A*) and mean readers' scores for individual anatomic structures and overall image quality (*B*). All scores were based on a 5-point Likert scale, comparing PCD-CT with EID-CT: 1 = inferior resolution with degraded visualization, 2 = slightly inferior resolution without affecting visualization, 3 = equivalent resolution and visualization, 4 = slightly superior resolution without affecting visualization, and 5 = superior spatial resolution with improved visualization.

FIG 2. Pöschl reformatted images in a patient with superior semicircular canal dehiscence, shown on EID-CT (*left*) and PCD-CT (*right*) images. The PCD-CT image (*B*) clearly demonstrates 2 discrete regions of dehiscence (*curved arrows*). These regions are also identifiable on conventional EID-CT (*A*), though the intact adjacent bone is less well-visualized. The integrity of the roof of the superior semicircular canal was not formally evaluated in the readers' study but is shown for illustrative purposes.

sided alternative. Matlab, Version r2015b (MathWorks), was used for statistical analysis.

RESULTS

Thirteen patients underwent a clinically indicated temporal bone scan using the ultra-high-resolution mode of EID-CT followed by an investigational PCD-CT scan, yielding 26 temporal bone datasets (including the left and right temporal bones) for comparison. The average age was 63.6 [SD, 13.4] years; 7 patients were women (Online Supplemental Data). The clinical indications for the CT examinations were hearing loss in 10 patients, ear fullness with concern for eustachian tube dysfunction in 1 patient, and otitis media with a perforated tympanic membrane in 1 patient. Two patients had a stapes prothesis in place from a prior surgery; 1 patient was status post resection of a vestibular schwannoma.

Figure 1 shows the neuroradiologists' comparison ratings for PCD-CT relative to EID-CT for each of the 7 critical anatomic structures. For PCD-CT images assessed by reader one, 47% of the images received a score of five, 39% received a score of 4, and 13% received a score of 3. Reader 1 gave a score of 2 for the incudomalleolar joint (slightly inferior resolution without affecting visualization) for 1 of 182 PCD-CT images and noted the presence of artifacts in the free text comment. For PCD-CT images assessed by reader two, 71% of the images received a score of five, 22% received a score of 4, and 7% received a score of 3.

Of the evaluated critical structures, the oval window received the highest mean reader score (4.79), followed by the incudostapedial joint (4.75). Additionally, the visualization of semicircular canal dehiscence was substantially enhanced on the PCD-CT Pöschl reformats as illustrated in Fig 2.

For overall image quality, PCD-CT received a mean score of 4.92 (SD, 0.27) for reader 1, and 4.54 (SD, 0.50) for reader 2, with PCD-CT found to be significantly better than EID-CT for overall image quality ($P < .001$). In 3 of 13 patients, the readers commented about the presence of minor artifacts (windmill effect in 1 patient) and slightly higher image noise (in 2 patients) on PCD-CT images; however, this did not substantially impact the visualization of critical structures (the PCD-CT overall image-quality score in these patients was ≥4 from both readers).

Images reformatted in oblique planes for illustrative purposes are shown in Figs 3–6. These images show the ability of PCD-CT to improve the visualization of ossicular anatomy (Fig 3), providing a more direct assessment of the incudostapedial joint (Fig 4), the anatomic relationship between a stapes piston and nearby structures (Fig 5), and the relationship between the anterior crus of the stapes and an area of otosclerosis (Fig 6).

DISCUSSION

This study represents one of the first in vivo, side-by-side comparisons of PCD-CT and EID-CT in temporal bone imaging. The results and the illustrative cases convincingly demonstrate the benefit of PCD-CT with 0.2-mm image thickness relative to an EID-CT with 0.4-mm image thickness for temporal bone imaging. In addition, a 31% decrease in the radiation dose was achieved due to the differences in the technologies. The 2 readers

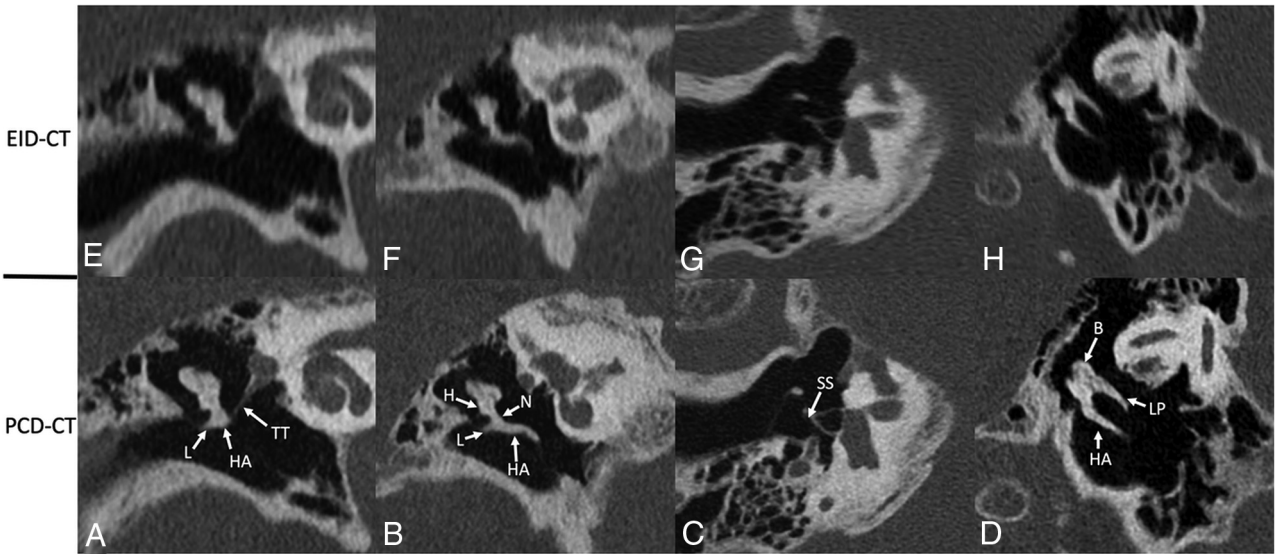

FIG 3. Ossicular anatomy, shown on conventional EID-CT (*upper row*) and PCD-CT (*lower row*). Reformatted images along the plane of the tensor tympani (*A* and *E*) demonstrate the tensor tympani (TT) extending to the upper handle of the malleus (HA); the lateral process (L) of the malleus is also clearly visible. An image reformatted along the long plane of the malleus (*B* and *F*) shows its handle (HA), lateral process (L), neck (N), and head (H). An image reformatted along the length of the stapes (*C* and *G*) clearly demonstrates the suprastructure (SS) and both crura. A "molar tooth" reformatted image (*D* and *H*) shows the HA of the malleus, as well as the body (B) and long process (LP) of the incus. These additional reformatted images were generated by a nonreviewer radiologist to demonstrate certain anatomic features but were not used by the readers to score image quality.

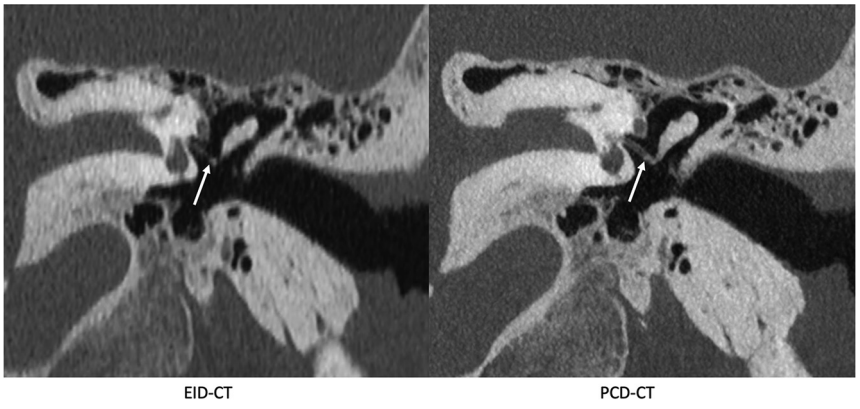

FIG 4. The incudostapedial joint (*arrows*), shown on EID-CT (*left*) and PCD-CT (*right*) images. The joint was one of several anatomic structures specifically graded using a 5-point Likert score, with higher scores favoring the quality of the PCD-CT images. The images reformatted in this plane were generated by a nonreviewer radiologist to demonstrate certain anatomic features but were not used by the readers to score image quality.

rated the PCD-CT images to be considerably sharper in multiple planes of reconstruction than those from the EID-CT scanner, which consequently improved critical structure visualization.

Prior studies have demonstrated noise reduction for temporal bone imaging using PCD-CT, as well as the radiologists' preference for PCD-CT images relative to EID-CT with an attenuating filter.[12,16,17] Leng et al[5] compared PCD-CT images with EID-CT images in a limited number of patients, covering examples from lung, joint, vascular, and temporal bone examinations. The authors reported a 21% noise reduction on PCD-CT temporal bone images, though only a single axial-plane image is shown as an example. A study using cadavers reported a 29% dose reduction in temporal bone imaging on a PCD-CT scanner, though also without reformatted examples.[16] These previous studies evaluated temporal bone images in axial planes at 0.25 mm, while the current study used a 0.2-mm section thickness in reformatted planes. The current study also demonstrated a 31% lower dose on PCD-CT relative to EID-CT. Further dose reduction could be achieved using a tin filter,[17,18] which was not available on the PCD-CT system at the time of this investigation.

On the basis of our results, we anticipate that PCD-CT will be especially advantageous in temporal bone imaging because precise evaluation of the anatomically complex region often requires optimized reformatted imaging at a high spatial resolution.[19] As shown in the illustrative cases of this pilot study, certain disease entities such as otosclerosis and superior semicircular canal dehiscence are much better demonstrated on PCD-CT images. In addition, the investigated PCD-CT technology will likely lead to improved evaluation of the ossicles in various planes due to reduced partial volume averaging enabled by the 0.2-mm section thickness. This improvement will allow better visualization of ossicular anomalies, postoperative changes related to ossicular prostheses, and the integrity of the incudostapedial articulation, among other aspects of temporal bone anatomy and postoperative findings.

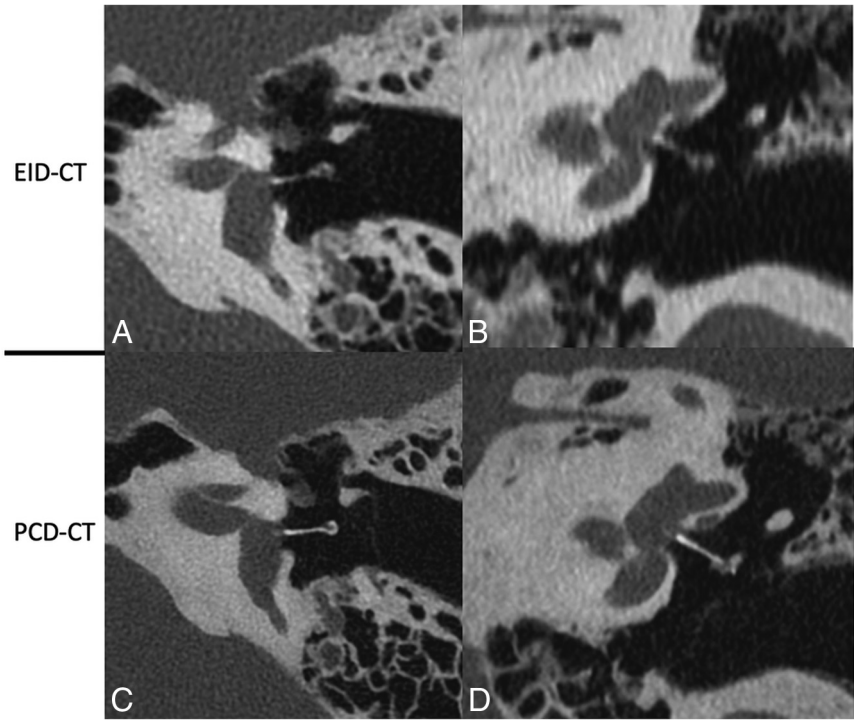

FIG 5. A stapes piston prosthesis shown on EID-CT (*upper row*) and PCD-CT (*lower row*) images. The prothesis is shown on oblique axial (*A* and *C*) and oblique coronal (*B* and *D*) reformats along the plane of the piston. In both planes, the stapes prosthesis was better delineated on PCD-CT due to reduced partial volume averaging from 0.2 mm sections. These additional reformatted images were generated by a nonreviewer radiologist to demonstrate certain anatomic features but were not used by the readers to score image quality.

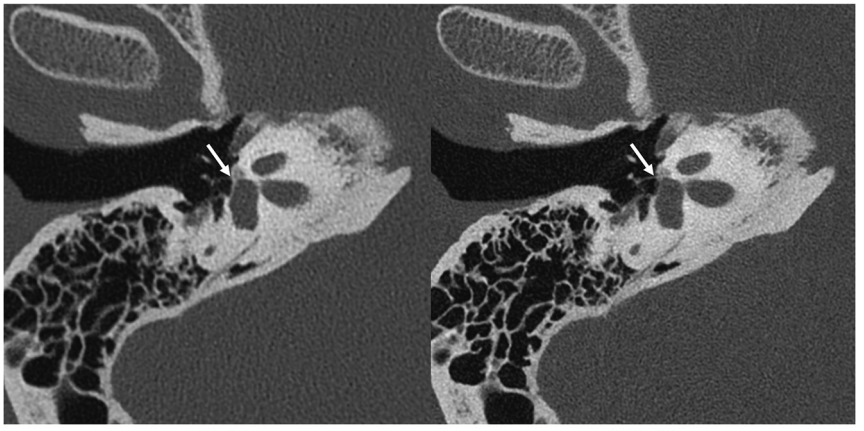

FIG 6. Images reformatted along the long axis of the stapes in a patient with fenestral otosclerosis shown on EID-CT (*left*) and conventional PCD-CT (*right*) images. The *arrow* points to the insertion of the anterior crus of the stapes into the region involved by otosclerosis. These additional reformatted images were generated by a nonreviewer radiologist to demonstrate certain anatomic features but were not used by the readers to score image quality.

The study had limitations. First, no independent reference standard was used in the readers' study for diagnostic truth. Instead, side-by-side blinded comparisons of PCD-CT and EID-CT images were performed, with scores assigned to 1 of the 2 modalities to assess the relative performance for image spatial resolution and visualization of critical structures. Because our primary goal in this study was to demonstrate improved spatial resolution and visualization from PCD-CT by leveraging sharper reconstruction kernels and a smaller section thickness (0.2 mm) not possible or available on EID-CT, we did not pursue aggressive dose-reduction strategies. Nonetheless, the overall image-quality score that reflects both image noise (a function of radiation dose) and sharpness showed that both readers favored PCD-CT images despite a 31% dose reduction.

CONCLUSIONS

The results of this patient study together with prior phantom and cadaveric studies suggest that PCD-CT offers substantial advantages over EID-CT with an attenuating filter for imaging the temporal bone. Temporal bone imaging seems particularly likely to benefit from the advantages of PCD-CT, given the submillimeter size of important anatomic structures.

ACKNOWLEDGMENTS

The authors thank Holly Kasten, Yong Lee, and Boleyn Andrist for patient recruitment and scanning and Elisabeth Shanblatt, PhD, for scanner support.

Disclosure forms provided by the authors are available with the full text and PDF of this article at www.ajnr.org.

REFERENCES

1. Willemink MJ, Persson M, Pourmorteza A, et al. **Photon-counting CT: technical principles and clinical prospects.** *Radiology* 2018;289:293–12 CrossRef Medline
2. Pourmorteza A, Symons R, Sandfort V, et al. **Abdominal imaging with contrast-enhanced photon-counting CT: first human experience.** *Radiology* 2016;279:239–45 CrossRef Medline
3. Flohr T, Petersilka M, Henning A, et al. **Photon-counting CT review.** *Phys Med* 2020;79:126–36 CrossRef Medline
4. Flohr TG, Stierstorfer K, Suss C, et al. **Novel ultrahigh resolution data acquisition and image reconstruction for multi-detector row CT.** *Med Phys* May 2007;34:1712–23 CrossRef Medline
5. Leng S, Rajendran K, Gong H, et al. **150-μm spatial resolution using photon-counting detector computed tomography technology: technical performance and first patient images.** *Invest Radiol* 2018;53:655–62 CrossRef Medline

6. Danielsson M, Persson M, Sjolin M. **Photon-counting x-ray detectors for CT.** *Phys Med Biol* 2021;66:03TR01 CrossRef Medline
7. Mannil M, Hickethier T, von Spiczak J, et al. **Photon-counting CT: high-resolution imaging of coronary stents.** *Invest Radiol* 2018;53:143–49 CrossRef Medline
8. Schmidt TG. **Optimal "image-based" weighting for energy-resolved CT.** *Med Phys* 2009;36:3018–27 CrossRef Medline
9. Do TD, Sawall S, Heinze S, et al. **A semi-automated quantitative comparison of metal artifact reduction in photon-counting computed tomography by energy-selective thresholding.** *Sci Rep* 2020;10:21099 CrossRef Medline
10. Zhou W, Bartlett DJ, Diehn FE, et al. **Reduction of metal artifacts and improvement in dose efficiency using photon-counting detector computed tomography and tin filtration.** *Invest Radiol* 2019;54:204–11 CrossRef Medline
11. Yu Z, Leng S, Kappler S, et al. **Noise performance of low-dose CT: comparison between an energy integrating detector and a photon counting detector using a whole-body research photon counting CT scanner.** *J Med Imaging (Bellingham)* 2016;3:043503 CrossRef Medline
12. Zhou W, Lane JI, Carlson ML, et al. **Comparison of a photon-counting-detector CT with an energy-integrating-detector CT for temporal bone imaging: a cadaveric study.** *AJNR Am J Neuroradiol* 2018;39:1733–38 CrossRef Medline
13. Rajendran K, Petersilka M, Henning A, et al. **Full filed-of-view, high-resolution, photon-counting detector CT: technical assistent and initial patient experience.** *Phys Med Biol* 2021;66:20 CrossRef Medline
14. Ferda J, Vendiš T, Flohr T, et al. **Computed tomography with a full FOV photon-counting detector in a clinical setting, the first experience.** *Eur J Radiol* 2021;137:109614 CrossRef Medline
15. Grunz JP, Huflage H, Heidenreich JF, et al. **Image quality assessment for clinical cadmium telluride-based photon-counting computed tomography detector in cadaveric wrist imaging.** *Int Radiol* 2021;56:785–90 CrossRef Medline
16. Leng S, Yu Z, Halaweish A, et al. **Dose-efficient ultrahigh-resolution scan mode using a photon counting detector computed tomography system.** *J Med Imaging (Bellingham)* 2016;3:043504 CrossRef Medline
17. Rajendran K, Voss BA, Zhou W, et al. **Dose reduction for sinus and temporal bone imaging using photon-counting detector CT with an additional tin filter.** *Invest Radiol* 2020;55:91–100 CrossRef Medline
18. Kim CR, Jeon JY. **Radiation dose and image conspicuity comparison between conventional 120kVp and 150kVp with spectral beam shaping for temporal bone CT.** *Eur J Radiol* 2018;102:68–73 CrossRef Medline
19. Juliano AF. **Cross-sectional imaging of the ear and temporal bone.** *Head Neck Pathol* 2018;12:302–20 CrossRef Medline